A Practical Control Approach for Safe Collaborative Supernumerary Robotic Arms

Mahdi Khoramshahi, Alexis Poignant, Guillaume Morel, Nathanael Jarrassé

▶ **To cite this version:**

Mahdi Khoramshahi, Alexis Poignant, Guillaume Morel, Nathanael Jarrassé. A Practical Control Approach for Safe Collaborative Supernumerary Robotic Arms. 2023 IEEE Conference on Advanced Robotics and its Social Impact (ARSO 2023), IEEE, Jun 2023, Berlin, Germany. hal-04067845

HAL Id: hal-04067845
https://hal.science/hal-04067845v1

Submitted on 13 Apr 2023

HAL is a multi-disciplinary open access archive for the deposit and dissemination of scientific research documents, whether they are published or not. The documents may come from teaching and research institutions in France or abroad, or from public or private research centers.

L'archive ouverte pluridisciplinaire **HAL**, est destinée au dépôt et à la diffusion de documents scientifiques de niveau recherche, publiés ou non, émanant des établissements d'enseignement et de recherche français ou étrangers, des laboratoires publics ou privés.

A Practical Control Approach for Safe Collaborative Supernumerary Robotic Arms

Mahdi Khoramshahi, Alexis Poignant, Guillaume Morel and Nathanael Jarrassé

***Abstract*— Supernumerary robotic arms have a high potential to increase human capacities to perform complicated tasks; e.g., having a third arm could increase the user's strength, precision, reachability, and versatility. However, having a robotic manipulator working in extreme proximity to the user raises new challenges in terms of safety; i.e., uncontrolled and hazardous collisions with the user's body parts and the environment. In this preliminary work, we show that most of these safety considerations can be extracted from standardized norms and translated into kinematics constraints for the robot. Thus, we propose a quadratic programming approach to achieve safe inverse-kinematics and physical interaction for supernumerary arms. We validate our approach in designing a safe supernumerary arm using the 7-Dof Kinova® Gen3 robot.**

I. INTRODUCTION

The Supernumerary Robotic Limbs (SRL) are wearable manipulators with the aim to increase humans' capacities to perform complex tasks through sensorimotor augmentation; e.g., to improve human strength, precision, versatility [1], grasping capacity [2], and perception [3]. Such extra artificial degrees of freedom can be added to the human body in several fashions: supernumerary arms [4], legs [5], fingers [6], tails [7], etc. These physical devices are intended to be lightweight with the possibility to be interfaced with human motor control; for example through brain-machine interfaces [8]. The first generation of SRLs were mostly weight-supporting devices, but the field progressed toward versatile, autonomous, and assistive SRLs. Currently, SRLs are applicable to industrial settings such as assembly lines [4], health-care where SRLs provide assistance for people with disabilities [9], surgical robotics [10], and many other domains; see [11] for a recent review.

In this work, we are concerned with redundant supernumerary arms with the goal to improve the manipulability –in its broad sense– of the human user. However, having such "third arms" poses new challenges when a powerful device operates in extreme proximity to the human-user. The risk of physical impacts that can lead to injuries raises new safety issues for SRLs. Most often, these issues are addressed from a mechatronic point of view [12]; e.g., by considering backdrivable motor, serials elastic actuators, advance sensing of contact, emergency stops for the actuators, etc. There is also a growing interest in utilizing intrinsically safe structures such as soft materials for wearable robots [13], [14]. However, relying fully on mechatronics and soft materials can severely limit the strengths and efficacy of SRLs. On the other hand, the safety issues of SRLs are less addressed from the control point of view [11] while there is a lack for a safe control framework in this literature; for instance, solving the Inverse Kinematics (IK) in a safe manner to avoid hazardous collision with the user, or destabilizing the user stability.

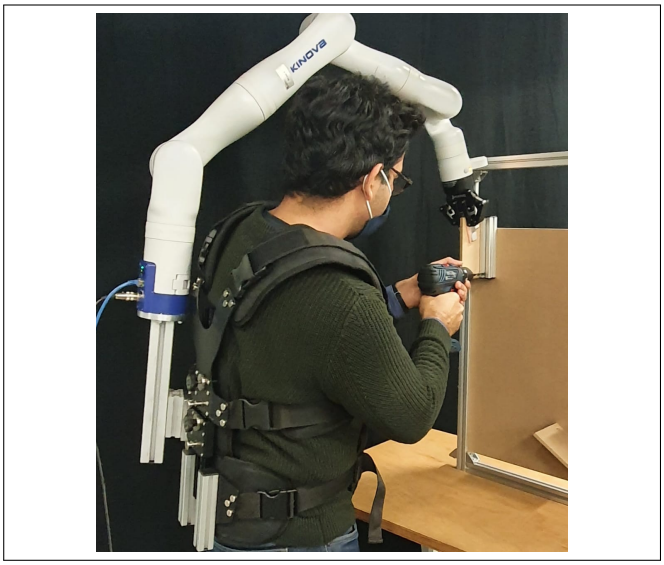

Fig. 1. Our robotic setup where the the Kinova® robot is worn using a vest. In this current setup, the power and the controller are off-board.

In this work, we consider a case in which the human-user provides input commands for the position of the end-effector (3 DoF) of a typical 7-DoF redundant robotic manipulator which leaves 4 DoF to satisfy the safety measures. In this manner, we reach an effective balance between the robot and human autonomy. To answer safety issues, we propose to use Quadratic Programming (QP) to solve the IK where the safety considerations can be embedded as inequality constraints for the robot joint velocities. QP is commonly used in the literature to safely generate impact in the environment [15], collision-free path planning for robotic applications [16], full-body IK of a humanoid robot with high DoF [17] or as a fast way to solve IK (to avoid computing pseudo inverse) [18]. Moreover, the QP approach is suitable for SRLs which require reactive motion planning; i.e., the robot needs to continuously react to human inputs and the interaction forces with the environment. Furthermore, we consider an admittance control loop to safely react to interaction forces [19], [20]. Nevertheless, obtaining quantified

This work is supported by H2020 FET NIMA project (899626).

All authors are with the Institute of Intelligent Systems and Robotics, Sorbonne Université, with CNRS UMR7222, and with INSERM U1150, Paris, France. khoramshahi@isir.upmc.fr

safety measures for SRLs is a challenge as well since there is no standardized or conventional approach in the literature. In this work, we propose to use the standardized ISO norms to extract inequality constraints for the QP solver. This enables our control architecture to provide a safe behavior for a supernumerary arm; i.e., to respect safety constraints on the workspace, the velocities, the interaction forces, and the impacts. To validate our approach, we use a commercial collaborative robot (7 DoF Kinova® Gen3 arm) is mounted on the back of the user.

II. METHOD

A. Robotic setup: hardware

The Kinova® Gen 3 Ultra lightweight robot L53 0007 is a CE-marked arm that is designed according to major safety standards. It fulfills several directives and standards such as Machinery Directive 2006/42/EC and ISO 12100:2010. Its power adapter cable is fitted with an integrated emergency stop (E-stop) button which is located near the experimenter and can be used to shutdown the robot. In case of a shutdown, the robot falls slowly due to the regenerative brakes. An additional emergency stop is also placed serially on an extension of the power cable and is placed close to the robot operator. As illustrated in Fig. 1 the robot is mounted on the back of the user. Similar setups can be found in the literature [12], [21]. Kinova Gen 3 is suitable for cobotics applications given its intrinsic mechanical properties [22]. Additionally, the native robot control library applies a number of different joint limits for safety purposes. This includes limits on joint position, speed, acceleration and torques. Gen3 also provides a low-level admittance control mode allowing a safe physical interaction with the environment. The native control library also monitors the feedback of the internal sensors of the robotic arm, along with the heat of internal components, and in case of faulty behavior, switches the robot to a safe compliant state. For the sensory information, we rely on the conventional robotic states; i.e., joint position, velocity, and torques. Beside a Robotiq two-finger gripper (2F-85) mounted on the end-effector, we do not use any other equipment such as sensors or tracking systems.

B. Control architecture

At the lowest level, a joint-velocity controller is provided by Kinova. To simplify the high-level control, we use a 3D joystick to command a desired velocity for the end-effector. To ensure a safe robotic execution of the human-commanded task, our mid-level controller needs to satisfy several constraints which are extracted from standardized norms. For instance, while moving the end-effector based on human commands, the robot needs to stay in a safe/designated workspace and avoid high-force exertion or high-power impacts. To this end, we propose a safe controller based on Quadratic programming. In this fashion, we solve the IK problem (converting human-user commands into proper joint velocities) while respecting different safety specifications. Given general safety specifications for pHRI and our specific scenarios, we compute a set of limits on different aspects of the robotic performance; i.e., workspace, joint positions, joint velocities, interaction forces, and mechanical power. These limits, along with the current robot's state, are used to compute a set of constraints for the QP-solver. This process is repeated in each time-step given the updated measurements and user's input which leads to a reactive behavior. Our mid-level controller is implemented in [23] which runs at 40 Hz. In case of a hard collision, the control is passed to the low-level admittance controller of the robot; i.e., the task and other ROS-dependent components will not affect the robot's behavior until the issue is resolved by the human-user. The QP problem is solved sequentially when the solution of each time-step serves as the warm-start for the next one. For this purpose, we use qpOASES library [24]. Some of the main technical parameters are set as follows: terminal tolerance $1e-5$, bound tolerance $1e-5$, max iteration $1e3$.

C. Constrained inverse kinematics using QP

We use a QP-based approach inspired by [25] to solve the following IK problem:

$$\begin{aligned} \min_{u,\delta} \quad & u^T W u + \delta^T Q \delta + g^T u \\ \text{s.t.} \quad & Ju + \delta = \dot{x}_d \\ & u_{min} < u < u_{max} \\ & \delta_{min} < \delta < \delta_{max} \\ & b_{min} < Au < b_{max} \end{aligned} \tag{1}$$

where the decision variables $u \in \mathbb{R}^n$ represents the joint velocity commands. W is a diagonal and positive semi-definite matrix representing the corresponding costs for moving each joint. We use $W = diag([0.1, 1, 10, 10, 1, 1, 1])$ which is chosen experimentally with high values for the 3rd and 4th joints as they affect the posture more than other joints. In the second term, $\delta \in \mathbb{R}^m$ represents the slack variables with its associated weight matrix $Q \in \mathbb{R}^{n \times n} \succ 0$ which is defined in a manner that $||Q|| >> ||W||$. For our implementation, we choose $Q = 1e8 I_n$ where I_n is the identity matrix of size n. We use the linear part ($g \in \mathbb{R}^n$) to favor an upright posture ($q_2 = 0$) in the null-space by choosing $g = [0, k_n q_2, 0, 0, 0, 0, 0]^T$ where q_2 is the position of the second joint, and k_n is the null-space stiffness. The goal of QP is to follow the desired end-effector velocity ($\dot{x}_d \in \mathbb{R}^m$) while respecting the safety constraints. The equality constraint represents the forward kinematics of the robot where $J \in \mathbb{R}^{m \times n}$ is the Jacobian matrix. It can be shown that neglecting the inequality constraints and the slack variables leads to the standard IK solution as:

$$u = J^{\#} \dot{x}_d + (I - J^{\#} J) \dot{q}_n \tag{2}$$

where $J^{\#} = W^{-1} J^T (J W^{-1} J^T)$ is the weighted Moore-Penrose pseudo-inverse and $\dot{q}_n = -g/2$ is the null-space velocity. In our control architecture, the desired velocity is computed as follows:

$$\dot{x}_d = \dot{x}_t + \dot{x}_a \tag{3}$$

Where the task-related velocities $\dot{x}_t \in \mathbb{R}^m$ are received from a high-level controller; e.g., a simple control interface using joystick or gaze. The second term $\dot{x}_a \in \mathbb{R}^m$ is generated by the admittance loop which handles the interaction forces with respect to soft and hard collisions.

D. Safety constraints for QP

In this section, we present how the safety measures for the robot are translated into the boundaries for the inequality constraints in the QP problem.

Velocity safety: ISO 10218-1:2011 [26] specifies that the maximum velocity of the robot end-effector should be 0.25m/s, to leave enough time to the operator to avoid or stop the robot. Therefore, we limit the commanded velocities for the EE at 0.2m/s. Furthermore, we limit the joint velocities at $\dot{q}_{max} = 0.3$rad/s to have reasonable linear velocities for other robotic parts. This is a conservative value that is reached experimentally. The QP inequality constraints for our decision variable constraints the joints velocities as follows:

$$-\dot{q}_{max} \leq u \leq \dot{q}_{max} \tag{4}$$

Angular position safeties: In order to take into account the mechanical limits of the robot, especially joint limits, we need to add angular position limits. However, as our command work is a velocity command, we need to express joint limits as velocity limits. To do so, we can set the following limits:

$$\frac{q_{min} - q}{p\Delta T} < u < \frac{q_{max} - q}{p\Delta T} \tag{5}$$

where q_{min} and $q_{max} \in \mathbb{R}^n$ are the angular joint limits, and ΔT is the control loop rate. $p > 1$ serves as a conservative factor; i.e., the robot will not violate the constraint even if the robot keeps the same velocity over the next p time-steps. Therefore, the higher p, the slower the joints move when they get close to their limits. We choose $p = 2$. The joint limits are experimentally set to $q_{min} = [-\infty, -120, -\infty, -120, -\infty, -120, -\infty]$ and $q_{max} = [\infty, 120, \infty, 120, \infty, 120, \infty]$ where ∞ refers to the fully-rotational joints. The inequalities in Eq. 4 and 5 lead to the following QP constraints:

$$\begin{cases} u_{min} = \max\{-\dot{q}_{max}, (q_{min} - q)/p\Delta T\} \\ u_{max} = \min\{\dot{q}_{max}, (q_{max} - q)/p\Delta T\} \end{cases} \tag{6}$$

Power safety: Average power consumption of Kinova® (45W [22]) respects ISO norms which defines 80W as the limit for cobots [26]. Furthermore, given the power at the end-effector as $\tau^T u$, we consider the following inequality constraint:

$$-P_{max} < \tau^T u < P_{max} \tag{7}$$

with $P_{max} = 4$W. This threshold is chosen experimentally by observing the value of $\tau^T u$ when the robot is operating satisfactorily in terms of resulting velocities and interaction forces. It is important to note that here we use the current torque measurement to estimate the power at the next time-step; i.e., assuming slow dynamics for interaction forces. In other words, the robot regulates its velocities based on the measured interaction forces. Moreover, we only limit the projected power at the end-effector and not for any other specific point on the robot body. Nevertheless, this is not a safety issue since there are other constraints at the joint-level.

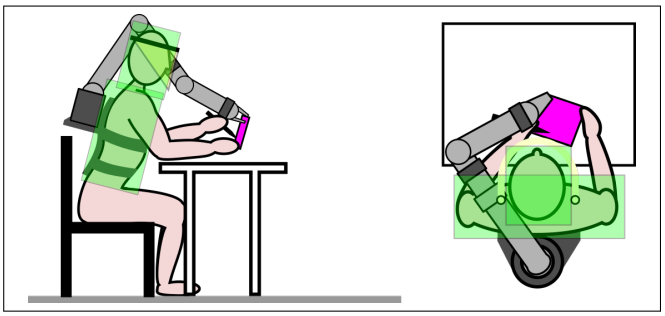

Fig. 2. View of the head and torso bounding boxes (in transparent green color) which are defined in the frame of the robotic arm base, i.e. the operator trunk.

Workspace safety: To avoid the collision between the wearable robot and its user, we model the human torso and head using bounding boxes as illustrated in Fig. 2. Here, we only consider collision avoidance with the user's head and torso. In other words, we allow physical interaction of the robot with the user's arms where its safety is handled via other parts of our mid-level controller. Using the QP constraints, we limit the robot's joints from entering these volumes. To this end, each bounding box is defined as a set of points $(X_{min}, X_{max}, Y_{min}, Y_{max}, Z_{min}, Z_{max})$ in the base frame. Here we assume that the user's torso and head movement with respect to the base of the robot is negligible considering a conservative choice for the size of the bounding boxes. We constraint the Cartesian velocity of each joint as follows:

$$\begin{cases} x_i + \dot{x}_i k\Delta t > x_i^+ & \text{if} \quad x_i > x_i^+ \\ x_i + \dot{x}_i k\Delta t < x_i^- & \text{if} \quad x_i < x_i^- \end{cases} \tag{8}$$

where x_i and $\dot{x}_i \in \mathbb{R}$ for $i = 1...n$ are the position and velocity of the ith joint of the robot. The upper and lower boundaries x_i^+ and $x_i^- \in \mathbb{R}^3$ are computed by aggregating the two bounding boxes. These constraints can be written as

$$\begin{cases} J_i u > (x_i^+ - x_i)/(k\Delta t) & \text{if} \quad x_i > x_i^+ \\ J_i u < (x_i^- - x_i)/(k\Delta t) & \text{if} \quad x_i < x_i^- \end{cases} \tag{9}$$

where $J_i \in \mathbb{R}^{n \times 3}$ for $i = 1...n$ are the partial Jacobians. These constraints are then added to the QP solver as a part of the A matrix; 3 constraints per joint. Furthermore, to have a conservative and damped behavior near the bounding boxes, we choose $k = 20$.

The inequalities in Eq. 7 and 9 lead to construction of the $A \in \mathbb{R}^{4n \times n}$ matrix and the corresponding boundaries for

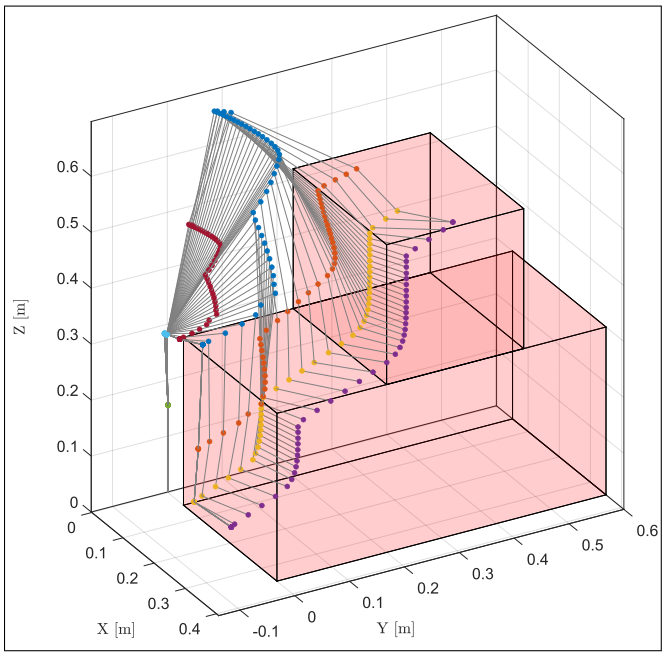

Fig. 3. The result of robot motion planning in avoiding the designated bounding boxes while following the desired end-effector velocities.

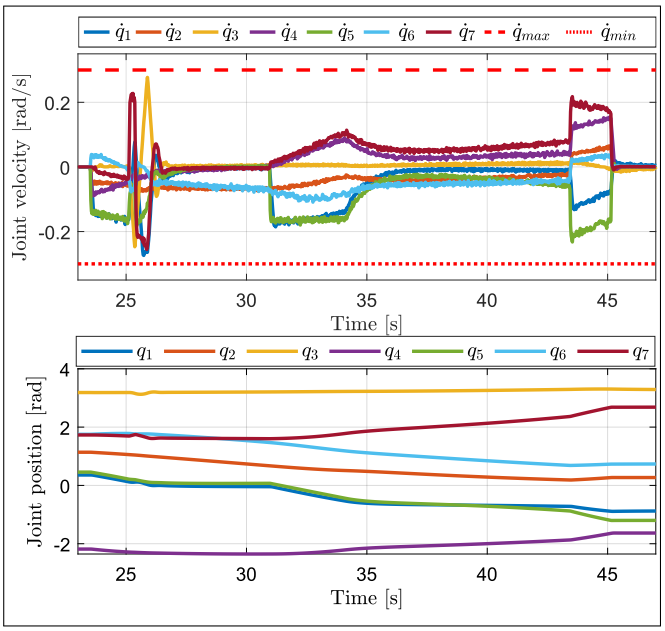

Fig. 4. The corresponding joints position and velocity for Fig. 3. The joint velocity limits are respected and the resulting joint positions are satisfactory in terms of smoothness. No collision or penetration into the bounding boxes occurs in this demonstration.

b_{min} and $b_{max} \in \mathbb{R}^{4n}$.

$$A = \begin{bmatrix} \tau^T \\ J_1 \\ \vdots \\ J_n \end{bmatrix}, \quad b_{min} = \begin{bmatrix} -P_{min} \\ \Gamma(x_1^+ - x_1)/(k\Delta t) \\ \vdots \\ \Gamma(x_n^+ - x_n)/(k\Delta t) \end{bmatrix} \tag{10}$$

where the switching function $\Gamma(x) = x$ for $x < 0$ and a large value otherwise in order to rend the constraint void. The computation for b_{max} is done similarly.

Collision safety: In order to provide a safe and versatile interaction with the environment, we handle the collisions at two levels; namely "soft" and "hard" collisions. Unlike the previous safety factors that were handled by the QP solver, collision safety is handled by the admittance loop. Soft collision is concerned with interaction forces that we expect from a safe physical interaction with the environment and humans; e.g., the human pushes the robot or when the robot physically manipulates an object. For this purpose, we use the following admittance feedback loop.

$$\dot{x}_a = \alpha J^{\dagger T} \Phi(\tau - \tau_g, \tau_{soft}) \tag{11}$$

where Φ is a deadzone function that is applied element-wise as follows:

$$\Phi_i(\tau, \tau') = \begin{cases} \tau_i - \tau_i' & \text{if} \quad \tau_i' < \tau_i \\ 0 & \text{if} \quad -\tau_i' < \tau_i < \tau_i' \\ \tau_i + \tau_i' & \text{if} \quad \tau_i < -\tau_i' \end{cases} \tag{12}$$

where $\tau' \in \mathbb{R}^n$ is an arbitrary vector with positive values. In our case, we choose $\tau_{soft} = [8, 6, 6, 6, 4, 4, 2]Nm$ which acts as the threshold below which no collision is detected. Moreover, τ_g is the estimated gravity effect and the measured torque on the ith joint respectively. $J^\dagger$ is the pseudo-inverse of the Jacobian. Here, α is the admittance gain that controls the behavior of the response (response time, stability, and oscillations); i.e., higher/lower α leads to lower/higher damping behavior. Therefore, in the case of a soft collision, this admittance rule moves the end-effector based on the interaction forces. This admittance loop also allows the user to indirectly control for the interaction forces through $\dot{x}_t$.

$$\begin{cases} F = K_v(\dot{x}_t + \dot{x}_a) \\ \dot{x}_a = \alpha F \end{cases} \tag{13}$$

This leads to

$$F = \frac{1}{1/K_v - \alpha} \dot{x}_t \tag{14}$$

where K_v is the forward gain imposed by the velocity controller. There, given high values for K_v, in interaction with the environment, $-\dot{x}_t/\alpha$ can be applied to the environment. However, this relation is only valid in a steady state while during the transient phases, these forces can be much higher, depending on the inertia and velocity of the robot. Therefore, it is crucial to consider a "hard" collision mode.

Hard collision: this mode classifies the abnormal collisions which might harm the human (or the robot). Such collisions are recognized by a higher level of force/torque (compared to the soft one). The implemented strategy is to stop the task (ignoring the desired end-effector motion) and render the robot fully compliant. To detect hard collisions, at each time-step, we check if any joint satisfies the following criterion:

$$|\tau - \tau_g| > \tau_{hard} \tag{15}$$

with $\tau_{hard} = [40, 40, 40, 40, 40, 40, 40]Nm$. Therefore, in case of a hard collision, we stop sending joint-velocity

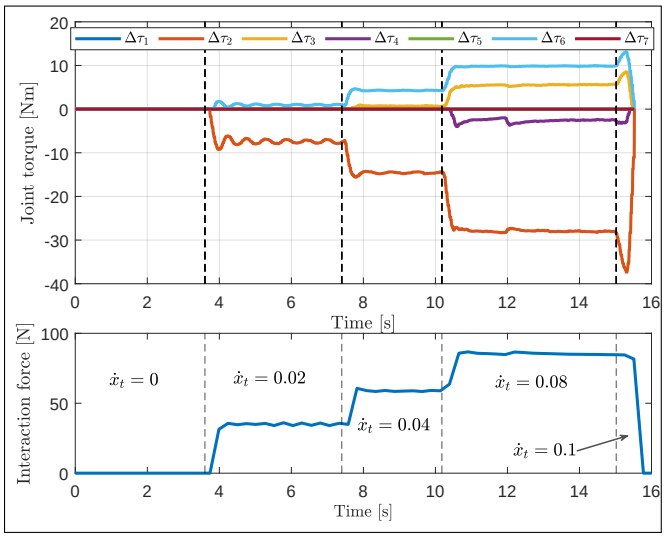

Fig. 5. The resulting behavior with respect to the interaction forces. The robot is initially placed in contact with a hard surface as the desired velocity ($\dot{x}_t$) increases over time. High interaction forces are recognized as hard collisions where the robot ignores the task and switches to a low-level admittance control.

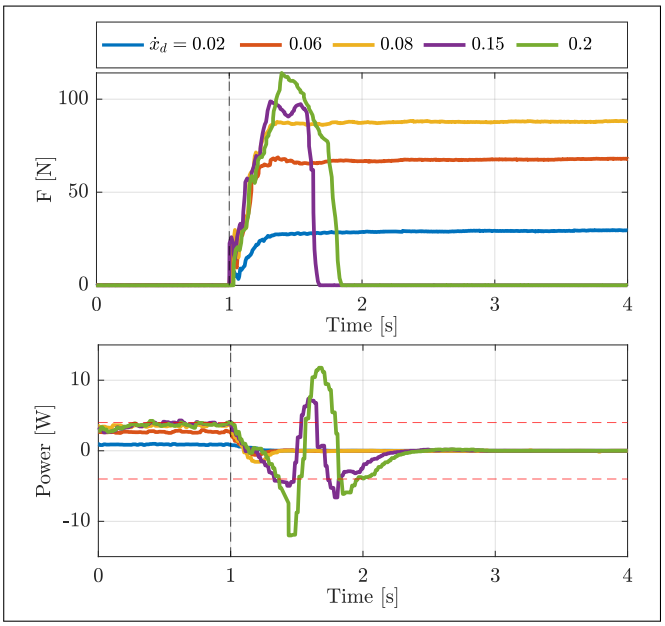

Fig. 6. The result of impacts when the robot collide with the environment at different speed. Higher velocities results in higher forces at the impact which is detected as hard collision and trigger the low-level admittance control. The plot of the power shows that this value remains in the boundaries before we switch to low-level admittance.

commands to the robot and switch the compliant mode implemented by Kinova® on the robot. The robot stays in this mode until the user specifies otherwise manually.

III. Results and Discussion

To validate our control architecture, we present two experimental scenarios. In the first scenario, we test the robot motion-planning in its joint space. To do this, we send a constant velocity for the end-effector ($\dot{x}_t = [0, .05, .02]$) while we expect the robot to avoid the bounding boxes and joint position and velocity limits. These results are illustrated in Fig. 3 with its corresponding joint position and velocity in Fig. 4. Given our choice for the slack variable, the robot is allowed to deviate slightly from the straight line in order to execute the task. Let us note that without the slack variable, the robot stalls when there is no solution for the QP problem. The size of the slack variable controls how much the robot's end-effector velocity can deviate from the desired one. This figure also shows that not only the end-effector but also all joints avoid penetrating into the bounding boxes. Such behavior allows the user to easily move the robot's end-effector around (via any arbitrary interface) without being worried about the robot's configuration and collision. In other words, the user is not required to 1) control all the joints individually, or 2) send precise commands to the end-effector. Furthermore, Fig. 4 illustrates other safety constraints were respected as well; i.e., joint velocities remain in the safe zone, and joint position limits are respected.

In the second experiment, we test the robot's behavior in terms of physical interaction with the environment. To this end, we put the robot's end-effector in physical contact with an external force sensor while we send different desired end-effector velocities to the robot. This result is depicted in Fig. 5 where we slowly increase the desired end-effector velocity (x_t from 0 to 0.2m/s). This increase in the desired velocity leads to an increase in the interaction forces between the robot and the environment. After a certain threshold around $F = 90$N which depends on τ_{hard} and the robot's configuration) the robot detects a hard collision and switches to the low-level admittance control which ignores the desired task. Thus the interaction forces disappear and the robot becomes compliant which allows the user to move the robot freely.

In the third experiment, we test the effect of impacts; i.e., the robot follows a constant desired velocity and collides with a hard surface. These results are illustrated in Fig. 6 which shows that a similar safety behavior to the previous figure is obtained; i.e., colliding with higher interaction forces triggers the low-level admittance control. The other subplot shows the projected power at the end-effector ($\tau^T \dot{q}$). We can see that before collision, this power remains inside the designated boundaries. The behavior of such power exchanges with the environment after the collision depends on the control mode. For the collisions with higher velocities ($\dot{x}_d = 0.15$ and 0.2), the low-level admittance control is triggered. We can see that this low-level controller is not constraining the power, however, providing a passive interaction with the environment. However, operating the robot using the QP in a safe range of velocities and interaction forces provide a satisfactory post-collision behavior. Finally, let us note that in the second and third experiments, we used a fixed-base configuration to be able to investigate the controller in physical interactions with rigid contacts. In the worn configuration, the situation is ameliorated given the compliance of the human body and the human ability to displace the robot's base.

IV. Conclusion

In this preliminary work, we presented a mid-level control strategy for a safe supernumerary robotic arm. We formulated our control as a constrained inverse kinematic problem that can be solved using Quadratic programming. We focused on two main safety considerations: workspace safety and interaction safety. These considerations were translated to inequality constraints for the QP problem; i.e., constraints on the commanded joint velocities. The upper/lower bounds of these constraints were extracted based on standardized safety norms. We experimentally validated our approach in a controlled laboratory environment. Our results show that such QP problems can be effectively solved which leads to a safe robotic behavior. Furthermore, we presented a generalized formulation that can be easily adapted to different robotic supernumerary arms. We provided guidelines and necessary details for each constraint to improve the reproducibility and adaptability of our controller. In our future work, we will exploit the information about the movement of the human-user to avoid dangerous or uncomfortable configurations; e.g., the risk of falling when the user bends forward with the robot extended forward as well. Furthermore, the human compensatory movements can be used for intention-recognition purposes and be used to improve the robot's autonomy and reactiveness; see our previous work on such control strategies [27–30].

References

[1] D. Gopinath and G. Weinberg, "A generative physical model approach for enhancing the stroke palette for robotic drummers," *Robotics and autonomous systems*, vol. 86, pp. 207–215, 2016.

[2] I. Hussain, G. Salvietti, L. Meli, C. Pacchierotti, D. Cioncoloni, S. Rossi, and D. Prattichizzo, "Using the robotic sixth finger and vibrotactile feedback for grasp compensation in chronic stroke patients," in *2015 IEEE International Conference on Rehabilitation Robotics (ICORR)*. IEEE, 2015, pp. 67–72.

[3] W. Wang, Y. Liu, Z. Li, Z. Wang, F. He, D. Ming, and D. Yang, "Building multi-modal sensory feedback pathways for srl with the aim of sensory enhancement via bci," in *International Conference on Robotics and Biomimetics*. IEEE, 2019, pp. 2439–2444.

[4] F. Parietti and H. H. Asada, "Supernumerary robotic limbs for aircraft fuselage assembly: body stabilization and guidance by bracing," in *2014 IEEE International Conference on Robotics and Automation (ICRA)*. IEEE, 2014, pp. 1176–1183.

[5] F. Parietti, K. C. Chan, B. Hunter, and H. H. Asada, "Design and control of supernumerary robotic limbs for balance augmentation," in *2015 IEEE International Conference on Robotics and Automation (ICRA)*. IEEE, 2015, pp. 5010–5017.

[6] I. Hussain, G. Salvietti, G. Spagnoletti, M. Malvezzi, D. Cioncoloni, S. Rossi, and D. Prattichizzo, "A soft supernumerary robotic finger and mobile arm support for grasping compensation and hemiparetic upper limb rehabilitation," *Robotics and Autonomous Systems*, vol. 93, pp. 1–12, 2017.

[7] H. Xie, K. Mitsuhashi, and T. Torii, "Augmenting human with a tail," in *Proceedings of the 10th Augmented Human International Conference 2019*, 2019, pp. 1–7.

[8] J. Eden, M. Bräcklein, J. Ibáñez, D. Y. Barsakcioglu, G. Di Pino, D. Farina, E. Burdet, and C. Mehring, "Principles of human movement augmentation and the challenges in making it a reality," *Nature Communications*, vol. 13, no. 1, pp. 1–13, 2022.

[9] L. Masia, I. Hussain, M. Xiloyannis, C. Pacchierotti, L. Cappello, M. Malvezzi, G. Spagnoletti, C. Antuvan, D. Khanh, M. Pozzi *et al.*, "Soft wearable assistive robotics: exosuits and supernumerary limbs," 2018.

[10] E. Abdi, E. Burdet, M. Bouri, and H. Bleuler, "Control of a supernumerary robotic hand by foot: An experimental study in virtual reality," *PloS one*, vol. 10, no. 7, p. e0134501, 2015.

[11] D. Prattichizzo, M. Pozzi, T. L. Baldi, M. Malvezzi, I. Hussain, S. Rossi, and G. Salvietti, "Human augmentation by wearable supernumerary robotic limbs: review and perspectives," *Progress in Biomedical Engineering*, vol. 3, no. 4, p. 042005, 2021.

[12] L. L. Z. Bright, "Supernumerary robotic limbs for human augmentation in overhead assembly tasks," Ph.D. dissertation, Massachusetts Institute of Technology, 2017.

[13] C. Walsh, "Human-in-the-loop development of soft wearable robots," *Nature Reviews Materials*, vol. 3, no. 6, pp. 78–80, 2018.

[14] P. H. Nguyen, I. I. Mohd, C. Sparks, F. L. Arellano, W. Zhang, and P. Polygerinos, "Fabric soft poly-limbs for physical assistance of daily living tasks," in *2019 International Conference on Robotics and Automation (ICRA)*. IEEE, 2019, pp. 8429–8435.

[15] Y. Wang, N. Dehio, A. Tanguy, and A. Kheddar, "Impact-aware task-space quadratic-programming control," *arXiv preprint arXiv:2006.01987*, 2020.

[16] Z. Wang, G. Li, H. Jiang, Q. Chen, and H. Zhang, "Collision-free navigation of autonomous vehicles using convex quadratic programming-based model predictive control," *IEEE/ASME Transactions on Mechatronics*, vol. 23, no. 3, pp. 1103–1113, 2018.

[17] S. Feng, E. Whitman, X. Xinjilefu, and C. G. Atkeson, "Optimization based full body control for the atlas robot," in *International Conference on Humanoid Robots*. IEEE, 2014, pp. 120–127.

[18] A. Escande, N. Mansard, and P.-B. Wieber, "Fast resolution of hierarchized inverse kinematics with inequality constraints," in *2010 IEEE International Conference on Robotics and Automation*. IEEE, 2010, pp. 3733–3738.

[19] V. Duchaine and C. Gosselin, "Safe, stable and intuitive control for physical human-robot interaction," in *International Conference on Robotics and Automation*. IEEE, 2009, pp. 3383–3388.

[20] A. Q. Keemink, H. van der Kooij, and A. H. Stienen, "Admittance control for physical human–robot interaction," *The International Journal of Robotics Research*, vol. 37, no. 11, pp. 1421–1444, 2018.

[21] A. S. Ciullo, M. G. Catalano, A. Bicchi, and A. Ajoudani, "A supernumerary soft robotic hand-arm system for improving worker ergonomics," in *International Symposium on Wearable Robotics*. Springer, 2018, pp. 520–524.

[22] Kinova. User guide: Kinova gen 3. [Online]. Available: https://www.kinovarobotics.com/product/gen3-robots

[23] Stanford Artificial Intelligence Laboratory et al., "Robotic operating system." [Online]. Available: https://www.ros.org

[24] H. J. Ferreau, C. Kirches, A. Potschka, H. G. Bock, and M. Diehl, "qpoases: A parametric active-set algorithm for quadratic programming," *Mathematical Programming Computation*, vol. 6, no. 4, pp. 327–363, 2014.

[25] W. Suleiman, "On inverse kinematics with inequality constraints: new insights into minimum jerk trajectory generation," *Advanced Robotics*, vol. 30, no. 17-18, pp. 1164–1172, 2016.

[26] "ISO 10218-1&2:2011, Safety requirements for industrial robots," International Organization for Standardization, Standard, 2011.

[27] M. Legrand, N. Jarrasse, E. de Montalivet, F. Richer, and G. Morel, "Closing the loop between body compensations and upper limb prosthetic movements: A feasibility study," *IEEE Transactions on Medical Robotics and Bionics*, vol. 3, no. 1, pp. 230–240, 2020.

[28] M. Legrand, N. Jarrasse, C. Marchand, F. Richer, A. Touillet, N. Martinet, J. Paysant, and G. Morel, "Controlling upper-limb prostheses with body compensations," in *International Symposium on Wearable Robotics*. Springer, 2020, pp. 101–106.

[29] M. Khoramshahi, G. Morel, and N. Jarrasse, "Intent-aware control in kinematically redundant systems: Towards collaborative wearable robots," in *2021 IEEE International Conference on Robotics and Automation (ICRA)*, 2021.

[30] M. Khoramshahi, A. Roby-Brami, R. Parry, and N. Jarrassé, "Identification of inverse kinematic parameters in redundant systems: Towards quantification of inter-joint coordination in the human upper extremity," *Plos one*, vol. 17, no. 12, p. e0278228, 2022.